Analysis of straight wire antenna by method of moments

Zhaoxian Zhou

***Abstract*— In this project, the classical straight wire antenna is analyzed by method of moments, both in frequency and time domains. Multiresolution analysis is also provided. We use Harr wavelets to compute adaptively the transient response of the straight wire antenna to a Gaussian pulse input electrical field.**

***Index Terms*— Computational electromagnetics, methods of moment, wire antenna, integral equation, transient analysis, multiresolution analysis.**

I. Introduction

WITH the outcoming of high-speed digital computers, computational electromagnetics is playing more and more important role in the electrical engineering. In the last several decades, a lot of researchers have been active in the field of computational electromagnetics. They have proposed Various numerical methods, such as finite-difference-time-domain (FDTD), finite element method (FEM) and methods of moment (MOM), to name a few. These methods have been applied successfully to a large variety of structures.

The most widely used numerical methods can be classified into some categories that deal with frequency-domain differential equations, time-domain differential equations, frequency-domain integral equations and time-domain integral equations, usually named FDDE, TDDE, FDIE and TDIE methods.

The large majority of integral-equation analysis of scattering has been in the frequency domain (FD), and the majority of differential-equation analysis has been in the time-domain (TD). IETD methods have been found to be unstable and highly expensive thus received less concern in the past. There is recently a growing interest in the time domain methods, with reasons being the increased concern in electromagnetic compatibility (EMC), electromagnetic pulse (EMP), and the ability to obtain broadband response with a single analysis, such as in antenna and radar cross section (RCS) problems. There are advantages of IETD methods over other methods. First, IE solvers only need the discretization of the scatterer surface rather than the volume, which results in a sharp decrease in the number of unknowns; second, IE methods automatically impose the radiation conditions on the integral equations, hence there is no need for absorbing boundary conditions that are required in the truncation of finite grids used in the DE methods. The most obvious disadvantage of the IE method may be that fact that a Green's function is needed at least for each class of problems, even same structures with different boundary conditions.

Zhaoxian Zhou is with the Computational Electromagnetics Laboratory, Department of Electrical and Computer Engineering, University of New Mexico. E-mail: zxzhou@eece.unm.edu.

Note that this paper is submitted as a term project for the "Computational electromagnetics" course, instructed by Prof. Christos Christodoulou.

The common issues in the IETD analysis are discretization of the surface and the fields, computation complexity and frequency scaling, algorithm stability, singular integrands and applications from PEC bodies to dielectric and lossy media. The main numerical analysis activity lies in the discretization of the body and the representation of the fields over it in a way that permits the integration.

The most famous method applied to the integral equations are method of moments. Basically, the method of moments transforms continuous integral equations into algebraic matrix equations. The discretizing process in essence involves the projection of the continuous operator (usually, the integro-differential operator) onto finite-dimensional subspaces defined by the basis and testing functions [1]. From this point of view, both finite element method and finite difference method are in some sense method of moments, or weighted-residual method.

The selection of basis and testing functions is the principal issue in the method of moments. Sub-domain functions are usually adopted because of their wide flexibility when applied to arbitrary computation domain. Their disadvantage is obvious. When extended to higher order approximation, all sub-domain functions usually change.

Recently, there have been active researchers working on wavelets and multiresolution analysis in electromagnetic applications. To name a few, there are Jameson [2], Sarker's group [3], [4], [5], Carin's group [6], [7], Katehi's group [8]. There are also other contributions [9], [10], [11], [12], [13], [14] and [15] as well.

Every method has its advantages and disadvantages. In this short paper, we will discuss only a small portion of the various computational methods in the scattering problem. Taking as an example of the straight wire scattering, the method of moments is dealt with here, both in frequency and time domains. As we are analyzing the transient response to a Gaussian pulse, we also provide the multiresolution analysis here. The multiresolution analysis (MRA) is proved to be very effective in the transient analysis, especially when dealing with multi-scale structures (the structures are smooth in the large portion but relatively rough in a small portion). The computational cost, both in time and storage, can be greatly reduced, if dealt with carefully.

After this brief introduction, we state the problem we are to analyze in section II. In section III, the formulae for our methods are derived. The numerical results are presented in section IV, followed by conclusions and discussions in the last section.

II. PROBLEM STATEMENT

Consider a straight thin wire antenna exposed to an input trans-magnetic (TM) electrical field. The wire is of diameter of 1 centimeter and length of 2 meters. The transient input electrical field is a Gaussian pulse,

$$\mathbf{E}^i(\mathbf{r},t) = \mathbf{E}_0 \frac{4}{T\sqrt{\pi}} e^{(-\gamma^2)}, \tag{1}$$

with

$$\gamma = \frac{4}{T}(ct - ct_0 - \mathbf{r}\cdot\mathbf{a_k}), \tag{2}$$

where $\mathbf{E}_0 = 120\pi\mathbf{a}_z, ct_0 = 3LM, \mathbf{T} = 2LM$, and $\mathbf{a}_k = -\mathbf{a}_x$.

We are to compute the current distribution induced on the wire and the transient current response at the center of the wire.

III. FORMULATIONS

In this section, we derive the formulations for the induced current along the thin wire. Assume a surface current distribution and a surface charge distribution along the thin wire, we can obtain the scattered fields. The boundary condition guarantees that on the perfect conductive surface, the incident fields and scattered fields sum up to zero, *i.e.*,

$$\mathbf{n}\times(\mathbf{E}^i + \mathbf{E}^s) = 0. \tag{3}$$

Corresponding formulations can be obtained both in frequency domain and time domain.

A. frequency domain formulation

The derivation in the frequency domain follows that in [16]. In the frequency domain, we have

$$\mathbf{E}^s = -j\omega\mathbf{A} - \nabla\Phi \tag{4}$$

$$\mathbf{A} = \mu \iint_S \mathbf{J}\frac{e^{-jkR}}{4\pi R} ds \tag{5}$$

$$\mathbf{\Phi} = \frac{1}{\epsilon}\iint_S \sigma\frac{e^{-jkR}}{4\pi R} dS \tag{6}$$

$$\sigma = \frac{-1}{j\omega}\nabla\cdot\mathbf{J} \tag{7}$$

We divide the thin wire into N segments. Approximating the integrals by summations and derivatives by finite differences, we get matrix equations as

$$\mathbf{ZI} = \mathbf{V}, \tag{8}$$

where matrices

$$\mathbf{I} = \begin{bmatrix} I(1) \\ I(2) \\ \vdots \\ I(N) \end{bmatrix} \tag{9}$$

$$\mathbf{V} = \begin{bmatrix} \mathbf{E}^i(1)\cdot\Delta\mathbf{l}_1 \\ \mathbf{E}^i(1)\cdot\Delta\mathbf{l}_1 \\ \vdots \\ \mathbf{E}^i(1)\cdot\Delta\mathbf{l}_N \end{bmatrix} \tag{10}$$

$$\mathbf{Z} = \begin{bmatrix} z_{11} & z_{12} & \cdots & z_{1N} \\ z_{21} & z_{22} & \cdots & z_{2N} \\ \vdots & & & \\ z_{N1} & z_{N2} & \cdots & z_{NN} \end{bmatrix} \tag{11}$$

where

$$z_{mn} = j\omega\mu\nabla\mathbf{l}_n\cdot\nabla\mathbf{l}_m\psi(n,m) + \frac{1}{j\omega\epsilon}\left[\Psi(n^+,m^+) - \Psi(n^-,m^+) - \Psi(n^+,m^-) + \Psi(n^-,m^-)\right] \tag{12}$$

and

$$\Psi n,m = \frac{1}{\Delta l_n}\int_{\Delta l_n}\frac{e^{-jkR_m}}{4\pi R_m} dl, \tag{13}$$

where n^-, n and n^+ denote the start, center and ending points of the n^{th} segments, respectively. The same applies to m^-, m and m^+.

Because

$$R_m = \begin{cases} \sqrt{\rho_m^2 + (z-z_m)^2} & m \neq n \\ \sqrt{a^2+z^2} & m = n \end{cases} \tag{14}$$

we have

$$\Psi(n,m) \approx \begin{cases} \frac{1}{4\pi\Delta l_n}\log\frac{\Delta l_n}{a} - \frac{jk}{8\pi} & m = n \\ \frac{e^{-jkR_{mn}}}{8\pi R_{mn}} & m \neq n \end{cases} \tag{15}$$

The frequency domain current for a specified frequency is thus computed by these formulae. To obtain the time domain current, iteration is needed for a lot of frequencies within the input spectrum. Then the inverse Fourier transform gives us the time domain current.

B. time domain formulation

Following the derivation in [17], directly from time domain Maxwell's equations,

$$\nabla\times\mathbf{E}(\mathbf{r},t) = -\mu\frac{\partial\mathbf{H}(\mathbf{r},t)}{\partial t}, \tag{16}$$

$$\nabla\times\mathbf{E}(\mathbf{r},t) = -\mu\frac{\partial\mathbf{H}(\mathbf{r},t)}{\partial t} + \mathbf{J}^i(\mathbf{r},t), \tag{17}$$

$$\nabla\cdot\mathbf{E}(\mathbf{r},t) = \frac{q_v^i(\mathbf{r},t)}{\epsilon}, \tag{18}$$

$$\nabla\cdot\mathbf{H}(\mathbf{r},t) = 0, \tag{19}$$

$$\nabla\cdot\mathbf{J}^i(\mathbf{r},t) = -\frac{\partial q_v^i(\mathbf{r},t)}{\partial t}, \tag{20}$$

time domain formulae can be derived.

By introducing the concept of vector and scalar potentials, we have the following equation relating the total electrical field $\mathbf{E}$ and vector potential $\mathbf{A}$:

$$\frac{\partial\mathbf{E}}{\partial t} = -\frac{\partial^2\mathbf{A}}{\partial t^2} + c^2\nabla(\nabla\cdot\mathbf{A}), \tag{21}$$

where $\mathbf{A}$ is in the retarded time integral form,

$$\mathbf{A}(\mathbf{r},t) = \mu\int_v \frac{\mathbf{J}^i(\mathbf{r},t-\frac{R}{c})}{4\pi R} dv'. \tag{22}$$

Applying to the 1-dimensional straight thin wire problem and assuming that the only induced current is in the axial z direction, we have only A_z component for the vector potential,

$$A_z(x,y,z,t) = \mu \int_{z'=-h}^{h} \frac{I(z', t-\frac{R}{c})}{4\pi R} dz', \quad (23)$$

where

$$R = \sqrt{x^2+y^2+(z-z')^2+a^2} = \sqrt{(z-z')^2+a^2}. \quad (24)$$

With the boundary conditions at the wire surface, the time domain formulation is derived:

$$\frac{\partial^2 A_z}{\partial z^2} - \frac{1}{c^2}\frac{\partial^2 A_z}{\partial t^2} = -\frac{1}{c^2}\frac{\partial E_z^i}{\partial t}, \text{ for } z \in (-h,h), \quad (25)$$

where

$$A_z(z,t) = \mu \int_{z'=-h}^{h} \frac{I(z', t-\frac{|z-z'|}{c})}{4\pi\sqrt{|z-z'|^2+a^2}} dz'. \quad (26)$$

The origin of the coordinate system lies at the center of the wire and $h = \frac{l}{2}$.

We divide the thin wire into $N+1$ segments with equal lengths and adopt pulse basis functions for the currents on the segments. Note, to satisfy the boundary conditions, we need to set currents on the end segments to zero for all time steps.

$$I \approx \sum_{k=1}^{N-1} I_k(t) f_k(z), \quad (27)$$

where the pulse function

$$f_m(z) = \begin{cases} 1 & z_m - \frac{\Delta z}{2} \le z < z_m + \frac{\Delta z}{2} \\ 0 & \text{otherwise} \end{cases} \quad (28)$$

Denoting $\kappa_{m,k}$ as the contribution of current on the k^{th} segment to the m^{th} segment,

$$\begin{aligned} \kappa_{m,k} &= \mu \int_{z'=z_k-\frac{\Delta z}{2}}^{z_k+\frac{\Delta z}{2}} \frac{1}{4\pi\sqrt{(z_m-z')^2+a^2}} dz' \\ &= \frac{\mu}{4\pi} \log\left(\frac{x_1}{x_2}\right) \end{aligned} \quad (29)$$

where

$$x_1 = z_m - z_k + \frac{\Delta z}{2} + \sqrt{\left(z_m - z_k + \frac{\Delta z}{2}\right)^2 + a^2}$$

$$x_2 = z_m - z_k - \frac{\Delta z}{2} + \sqrt{\left(z_m - z_k - \frac{\Delta z}{2}\right)^2 + a^2}.$$

we can write the integrals as summations,

$$\begin{aligned} A_{m,n} &= \mu \int_{z'=-h}^{h} \frac{I(z', t-\frac{|z_m-z'|}{c})}{4\pi\sqrt{(z_m-z')^2+a^2}} dz' \\ &\approx \mu \int_{z'=-h}^{h} \frac{\sum_{k=1}^{N-1} I_k(t_n - \frac{|z_m-z'|}{c}) f_k(z')}{4\pi\sqrt{(z_m-z')^2+a^2}} dz' \\ &= \sum_{k=1}^{N-1} I_k\left(t_n - \frac{|z_m-z'|}{c}\right)\kappa_{m,k} \\ &= I_{m,m}\kappa_{m,m} + \bar{A}_{m,n} \end{aligned} \quad (30)$$

where

$$\bar{A}_{m,n} = \sum_{k=1,k\neq m}^{N-1} I_k\left(t_n - \frac{|z_m-z'|}{c}\right)\kappa_{m,k} \quad (31)$$

are the vector potentials from the known currents obtained from previous steps.

Approximating the derivatives in equation 25 by central finite differences, we obtain

$$\begin{aligned} &\frac{A_{m+1,n} - 2A_{m,n} + A_{m-1,n}}{(\Delta z)^2} - \frac{A_{m,n+1} - 2A_{m,n} + A_{m,n-1}}{(c\Delta z)^2} \\ &= -F_{m,n} \end{aligned} \quad (32)$$

where

$$F_{m,n} = \frac{1}{c^2}\frac{\partial E_z^i(z_m,t_n)}{\partial t}. \quad (33)$$

In the explicit case, where $\frac{c\Delta t}{\Delta z} \le 1$, we have $I_{m,n}\kappa_{m,m}$

$$\begin{aligned} &= -\bar{A}_{m,n} + 2A_{m,n-1} - A_{m,n-2} + (c\Delta t)^2 F_{m,n-1} \\ &+ \left[\tfrac{c\Delta t}{\Delta z}\right]^2 (A_{m+1,n-1} - 2A_{m,n-1} + A_{m-1,n-1}] \end{aligned} \quad (34)$$

By selecting $\frac{c\Delta t}{\Delta z} = 1$, we simplify the equation to

$$\begin{aligned} I_{m,n}\kappa_{m,m} &= -\bar{A}_{m,n} + (c\Delta t)^2 F_{m,n-1} \\ &+ A_{m+1,n-1} + A_{m-1,n-1} - A_{m,n-2} \end{aligned} \quad (35)$$

Note that the currents at the end segments are always set to be zero.

By these equations, we can compute the induced currents segment by segment in space, step by step in time.

C. multiresolution analysis in time domain

Multiresolution analysis is rather important in computational electromagnetics, especially in transient analysis or structures with multiple scales.

In this project, we use extended Harr wavelet basis to decompose the unknown induced current. First, we compute the induced current at a lower resolution level N.

$$I(z,t) = I_0(t)\Phi(z) + \sum_{s=1}^{N}\sum_{k=1}^{s-1} \Psi_{sk}(z) I_{sk}(t) \quad (36)$$

where $\Phi(z)$ is the scaling function and $\Psi_{sk}(z)$ is the wavelet function. s is the scale index and k is the dilation index.

The domain is divided into 2^N+1 uniform segments, with $\Delta z = \frac{1}{2^N+1}$. Note that we need to set the currents at the ends to be zero to satisfy the boundary conditions. We write the equivalent length that the basis functions span as

$$l_{eq} = \frac{l}{2^N+1} 2^N \quad (37)$$

The basis functions are defined as

$$\Phi(z) = \begin{cases} 1 & 0 \le z < l \\ 0 & \text{otherwise} \end{cases} \quad (38)$$

and

$$\Phi_{sk}(z) = \begin{cases} 1 & \frac{l_{eq}}{2^s}(2k-2) \le z < \frac{l_{eq}}{2^s}(2k-1) \\ -1 & \frac{l_{eq}}{2^s}(2k-1) \le z < \frac{l_{eq}}{2^s}2k \\ 0 & \text{otherwise} \end{cases} \quad (39)$$

We denote the central points of the N segments (except the half segment at each end) as $z(i)$, where $i = 2, 3, ..., N+1$, then

$$A_{m,n} = \mu \int_{z'=0}^{l_{eq}} \frac{I(z', t - \frac{|z_m - z'|}{c})}{4\pi\sqrt{(z_m - z')^2 + a^2}} dz' \tag{40}$$

For the low frequency (scaling function) term,

$$\frac{\mu}{4\pi} \int_{z=0}^{l_{eq}} \frac{I_0(t_n - \frac{|z' - z_m|}{c})}{\sqrt{(z' - z_m)^2 + a^2}} \Phi(z') dz'$$

$$= \frac{\mu}{4\pi} \sum_{i=2}^{2^N+1} I_0(n - \frac{|m-i|\Delta z}{c\Delta t}) \int_{z_i - \frac{\Delta z}{2}}^{z_i + \frac{\Delta z}{2}} \frac{dz'}{\sqrt{(z' - z_m)^2 + a^2}}$$

$$= \sum_{i=2}^{2^N+1} \kappa_{mi} I_0(n - |m-i|) \tag{41}$$

for $m = 1, 2, 3, ..., 2^N + 1$, and κ is defined in equation 29.

For the wavelet terms,

$$\frac{\mu}{4\pi} \int_{z=0}^{l_{eq}} \frac{I_0(t_n - \frac{|z' - z_m|}{c})}{\sqrt{(z' - z_m)^2 + a^2}} H_{sk}(z') dz'$$

$$= \sum_{i=2^{N-s}(2k-1)+1}^{2^{N-s}(2k-2)+2} I_{sk}(n - |m-i|) \kappa_{mi} - \sum_{i=2^{N-s}(2k-1)+1}^{2^{N-s}(2k)+1} I_{sk}(n - |m-i|) \kappa_{mi} \tag{42}$$

for $m = 1, 2, 3, ..., 2^N + 1$.

Thus, writing

$$A1 = \sum_{i=2}^{2^N+1} \kappa_{mi} I_0(n - |m-i|) + \sum_{s=1}^{N} \sum_{k=1}^{2^{s-1}} \tag{43}$$

$$A2 = \sum_{i=2^{N-s}(2k-2)+2}^{2^{N-s}(2k-1)+1} I_{sk}(n - |m-i|) \kappa_{mi} - \sum_{i=2^{N-s}(2k-1)+1}^{2^{N-s}(2k)+1} I_{sk}(n - |m-i|) \kappa_{mi} \tag{44}$$

and κ is defined as in equation 29.

we have

$$A(m,n) = A1 + A2 = \alpha_m \cdot I_n + \bar{A}_{mn} \tag{45}$$

where dimensions of matrix α_m are 1×2^N; $\bar{A}_{mn}$ is the vector potential computed by the currents no later than time step $n-1$ and defined as in equation 31.

Note that if we choose $\frac{c\Delta t}{\Delta z} = 1$, the matrix α_m has only $N+1$ non-zero elements.

Equation 25 can be written in the form of

$$\alpha \cdot I_n = B \tag{46}$$

Matrix α, with dimensions of $\frac{N}{2} \times \frac{N}{2}$, is a special sparse matrix. Its inversion needs linear time. Matrix I_n, with dimensions of $\frac{N}{2} \times 1$, is the scaling and wavelets coefficients at the time step n. Matrix B is also $2^N \times 1$. Its component B_m can be computed by

$$B_m = -\bar{A}_{m,n} - A_{m,n-2} + F_{m,n-1} + A_{m+1,n-1} + A_{m-1,n-1} \tag{47}$$

Thus far, we have computed the induced currents at a lower resolution N, by moment methods directly from choosing extended Harr scaling function and wavelets as basis functions. It is well known that there exist relationship between the Harr basis functions and the ordinary pulse basis functions. There is sparse matrix that can transform Harr basis functions into pulse basis functions, and vice versa.

Our task is to analyze the transient response of the straight thin wire to a Gaussian pulse electrical field. We know that at the early stage of the response, the induced current is large because of the input field, while at later time, the induced current attenuates as the energy radiates into the space. In the early time, the induced current follows mostly the frequency characteristics of the input Gaussian pulse. As the input field ceases, the inherent resonant property of the wire antenna dominates.

It is reasonably to come to the conclusion that at different time steps of the simulation, and at different positions along the wire, we may need different basis functions. In our problem, where the input Gaussian field is a uniform plane wave, the induced current exhibits a sinusoidal waveform along the length of the wire.

The first scene is very clear. At the time when induced current shows extremes, we need more basis functions to characterize it, while when the current is almost zero along the whole wire, we need less, (even only the scaling function) basis functions. Our case is not a good exhibition for the second point. If the input pulse does not extend to the whole length of the wire like the uniform plane wave does, or if we imagine that the straight wire is somewhat inclined to the input that the input pulse reaches different portions of the wire at different time, the movie is vivid: the induced current exhibits a moving pulse along the wire.

This is actually a 2-dimensional application of wavelet basis functions. The length of the wire is one dimension and the time is another. We can apply directly to it the moment methods by using 2-dimensional Harr wavelet basis functions. The question is, when we deal with the retarded time problem in the time domain, it is not easy to use full domain basis functions in the marching-on-time (MOT) methods. Thus in this paper, we try to analyze it in a simple $1\frac{1}{2}$-D manner. That is, on the time axis, we choose pulse basis functions. For each time step, we choose Harr basis functions based on the real-time induced currents. For example, at the current time step, we can choose resolution N_1, while at next time step, we may choose resolution N_2. Because we are choosing explicit method to compute the current, and we have chosen $c\Delta t = \Delta z$, the time step varies with the resolution adopted along the length of wire.

We need to set up criteria for adaptive determination when in time step and where on the lower order segments along the wire we need higher order basis functions.

First, we apply the adaptivity along the time axis. Suppose at time step n, we have computed the basis functions up to level

N. Denote the matrix of coefficients of the basis functions as

$$\alpha = \begin{bmatrix} c_{0,0}(n) \\ c_{1,1}(n) \\ c_{2,1}(n) \\ c_{2,2}(n) \\ \vdots \\ c_{N,1}(n) \\ \vdots \\ c_{N,2^{N-1}}(n) \end{bmatrix}. \quad (48)$$

We set up a tolerance such that all the elements in matrix α that are less than the tolerance be considered as zero. If the sparsity of the matrix α is small, it is necessary to upgrade to higher level wavelets. Otherwise, if the sparsity is large enough, we can adopt lower level basis functions, or with other considerations, we can keep the same level of resolution. Note that when we adopt a higher order resolution, the currents computed at previous time steps should be up-sampled for the reason that we always adopt an explicit algorithm in the computation of vector potentials A and $\bar{A}$. Similarly, when a lower resolution is adopted, the previous currents are down-sampled. We use interpolation method to perform the task. Based on the sinusoidal current waveform along the wire, second order spline interpolation gives better accuracy than linear interpolation.

Second, we determine where along the wire, higher order basis functions are needed. The method adopted here is described as below. We double the number of nodes first. The vector potential at each node is interpolated based on the computed values at order N. An error function is selected as

$$\begin{aligned} ERR_{m,n} &= \frac{A_{m+1,n} - 2A_{m,n} + A_{m-1,n}}{\Delta z^2} \\ &\quad - \frac{A_{m,n+1} - 2A_{m,n} + A_{m,n-1}}{(c\Delta z)^2} \\ &\quad + F_{m,n} \end{aligned} \quad (49)$$

By setting a tolerance, we can determine, when and where along the wire, we need a higher order wavelet basis.

Suppose at time step n, a higher order $(N+1)$ wavelet basis is needed and its dilation index m (in another word, the position along the length of the wire) is determined. Next, we try to compute the coefficient $I_{N+1,m}(n+1)$ for the wavelet basis $\Psi_{N+1,m}(z)$ at time step $n+1$.

If we still use explicit method and select $\frac{c\Delta t}{\Delta z} = 1$, we need to cut Δt to half because Δz is halved in the case.

Assume the two new nodes at segment m are denoted as z_{m_1} and z_{m_2}. By applying equation

$$A_{m,n} = -A_{m,n-2} + (c\Delta t)^2 F_{m,n-1} + A_{m+1,n-1} + A_{m-1,n-1} \quad (50)$$

to node z_{m_1}, after two iterations, we obtain the higher order coefficient

$$I_m(n+1) = \frac{1}{\kappa'_{m_1,m_1}} \left[T_1 + \left(\frac{\kappa'_{m_1,m_2}}{\kappa'_{m_1,m_1}} - 1 \right) T_2 \right] \quad (51)$$

where

$$T_1 = A_{m-1,n} - A_{m,n+1} + (c\Delta t)^2 F_{m,n} \quad (52)$$

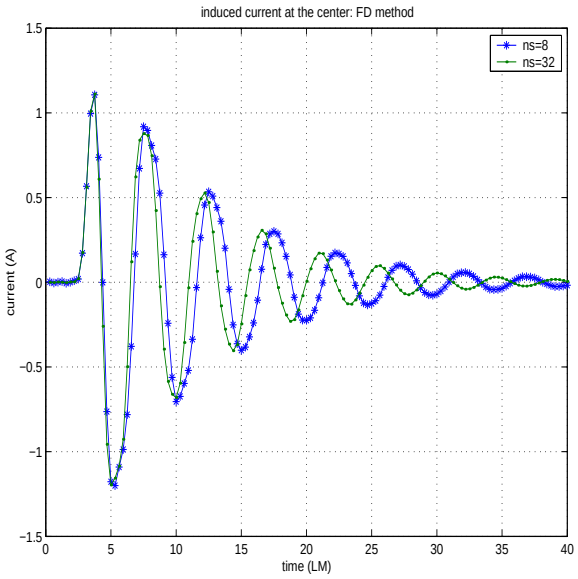

Fig. 1. Induced current with time at the center of the wire: FD method, computed at 128 uniformly spaced frequencies, then take the inverse Fourier transform.

and

$$T_2 = A_{m-1,n} - A_{m,n-1} + (c\Delta t)^2 F_{m,n} \quad (53)$$

Similarly, applying equation 50 to node z_{m_2}, we have

$$I_m(n+1) = \frac{1}{\kappa'_{m_2,m_2}} \left[T_1 + \left(\frac{\kappa'_{m_2,m_1}}{\kappa'_{m_2,m_2}} - 1 \right) T_2 \right] \quad (54)$$

where

$$T_1 = A_{m,n+1} - A_{m+1,n} - (c\Delta t)^2 F_{m,n} \quad (55)$$

and

$$T_2 = A_{m,n-1} - A_{m+1,n} - (c\Delta t)^2 F_{m,n} \quad (56)$$

By averaging equations 51 and 54, we obtain the coefficient for the higher order wavelet. Especially, in our case, the wire shows symmetry, the equation is thus simplified to

$$I_m(n+1) = \frac{\kappa'_{m_1,m_2}}{2\kappa'^2_{m_1,m_1}} (A_{m-1,n} - A_{m+1,n}) \quad (57)$$

IV. Numerical results

The input electrical field is expressed in equations 1 and 2. Based on Fourier transform pairs

$$X(f) = \int_{-\infty}^{\infty} x(t) e^{-j2\pi ft} dt; \quad (58)$$

and

$$X(t) = \int_{-\infty}^{\infty} X(f) e^{j2\pi ft} df, \quad (59)$$

its frequency domain representation is

$$\mathcal{F}(\mathbf{E}^i) = \mathbf{E}_0 \frac{1}{c} e^{(-\frac{\pi T f}{4c}^2)} e^{-j2\pi f t_0} \quad (60)$$

$\mathbf{E}_0 = 120\pi \mathbf{a}_z, ct_0 = 3LM, \mathbf{T} = 2LM$, thus, 90% of its spectrum lies in the region of $0 \sim 300MHz$. We choose 128 uniformly distributed frequency points within the spectrum, compute the induced currents, then take the inverse Fourier

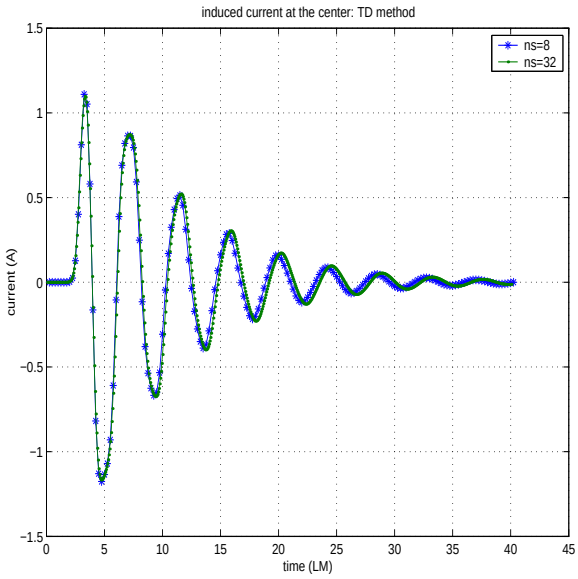

Fig. 2. Induced current with time at the center of the wire: TD method, using pulse basis functions, explicit MOT method.

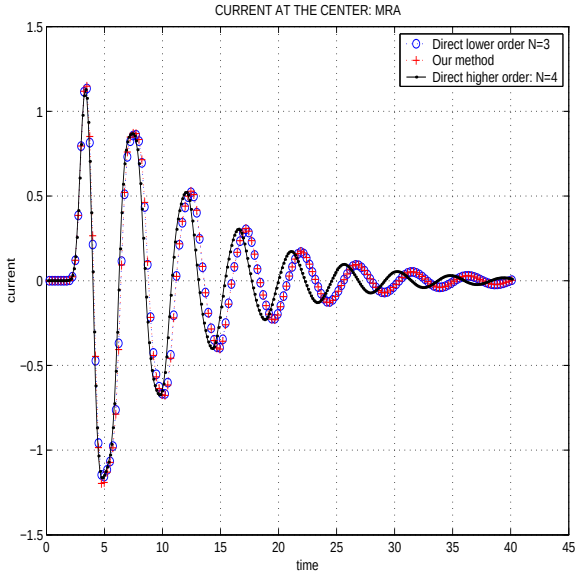

Fig. 3. Transient current at the center of the wire computed by different resolutions: TD method, using Harr wavelet basis functions at different resolutions. Using linear interpolation in adaptive method.

transform to obtain the time domain current for each segment along the wire. In the frequency domain method, We adopt the equations illustrated in equation 8 and those follow. The induced current at the center of the wire is illustrated in figure 1 for cases of dividing the whole wire into 8 and 32 segments.

The time domain method used to compute the induced current is expressed in equation 35. Note we use explicit method here. That means, we can compute the currents in a marching-on-time (MOT) manner, instead of solving a non-diagonal matrix equation in the implicit method. Similarly, the induced current at the center of the wire is illustrated in figure 2 for cases of dividing the whole wire into 8 and 32 segments.

In the multiresolution method, we want to derive a method by which less computation time could lead to better accuracy. The formulae described in the last section, in fact, adopt interpolation method in some sense, to obtain the higher order results. For our case, the improvement looks not as good as it should be. The possible reasons are (1.) in the derivation of the formulae, for each segment, we used two iterations to reach the higher order results from the lower order. We have not considered the effects of the new coefficients from other segments; (2.) in our case, the structure shows symmetry, the interpolation procedure provides the least improvement at the center of the wire. Hence the observed transient currents at the center of the wire, showed in figure 3, are almost the same as the lower order results.

We found in figure 3 that there is a time delay between the induced transient currents computed by the lower and higher order resolutions. Comparing the results from different resolutions, we found the fact that the result converges as the resolution level increases. A reasonable explanation to this phenomenon is that at the early time, the response is dominated by the input frequency spectrum while at the later time the response exhibits the resonant characteristics of the wire antenna. In our example, the input spectrum is around about 150 MHz. The wire antenna's resonant frequency is about 75 MHz. The physical length of the wire is about one wavelength of the input field or about half wavelength of the resonant frequency. Based on experience, the lowest resolution that gives satisfactory accuracy is $N = 4$ (that is 16 uniform segments along the wire). We found that for this problem, resolution $N = 6$ (64 segments) would give converged results.

Usually, we can obtain results in higher order resolutions by adding some higher order wavelet basis functions to the lower order basis. But in our case, where there exists a lagging phenomena between results in different resolutions, we can not obtain satisfactory results in higher order resolutions by just adding some higher order coefficients without changing the lower order coefficients. The results computed directly from pulse basis functions at different resolutions can be transformed, with a small portion of the computation time, into results adopting wavelet basis functions. It can be easily seen that the coefficients for lower order basis functions changed from lower order to higher order resolutions. Thus, it is necessary to re-calculate the coefficients of all the basis functions instead of just the added higher order basis functions.

we analyze the simplest case first. At time step n, we take different procedure based on the density of the coefficient matrix. If the coefficient matrix is dense enough (we set each coefficient not exceeding a preset tolerance to zero), we double the number of segments along the length of the wire at next time step. That means, we adopt the next higher resolution for all the segments along the wire; if the density is small enough, we adopt a lower order resolution; otherwise, we keep the current resolution to compute the induced current for the next step.

For one set of tolerances, we showed the induced currents in figure 4. It is observed that there exist non-smoothness when the algorithm is in transition between different resolution levels (especially in continuous transitions). To eliminate this effect, it is recommended that the transition between resolu-

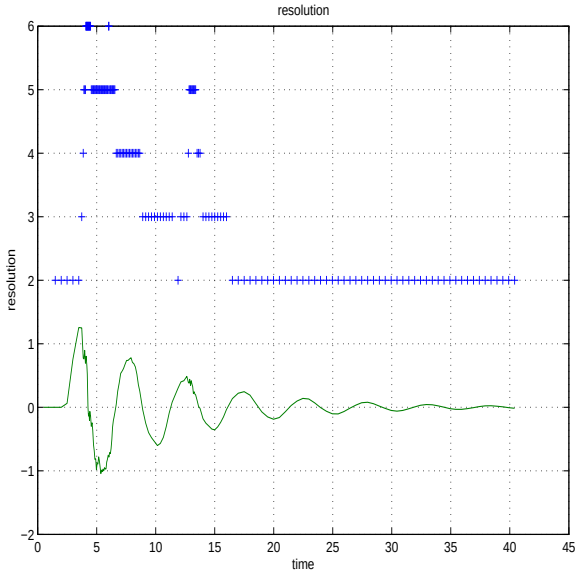

Fig. 4. Adaptive computation of transient current at the center of the wire. The set of tolerances makes the transition between different resolution levels rather sensitive.

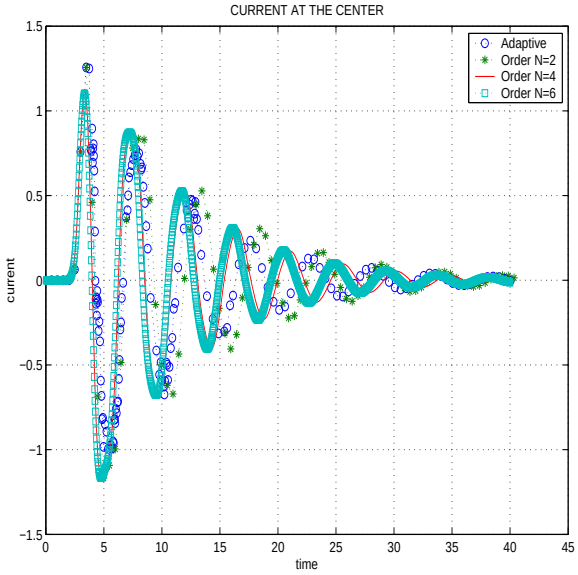

Fig. 6. transient current at the center of the wire: adaptive method compared with fixed resolution

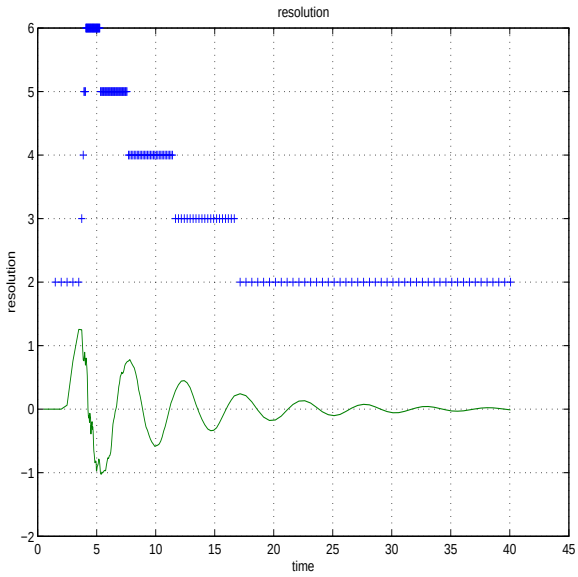

Fig. 5. Adaptive computation of transient current at the center of the wire: different set of tolerances makes the transition less sensitive.

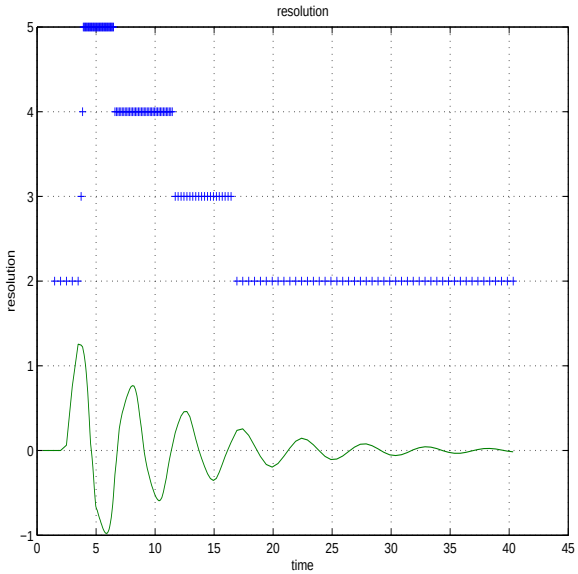

Fig. 7. transient current at the center of the wire: adaptive method (spline interpolation)

tions not be too frequent. Another result as in figure 5 shows the improvement around time $13LM$. The result is much smoother.

We compute the induced currents with adaptive resolution and fixed resolutions $N = 2, 4, 6$. In the adaptive method, we adopt the same configuration as that adopted in figure 4. The comparison is showed in figure 6. It can be easily found that at the very early stage, the induced current is ignorable and thus the adaptive method adopts the lowest resolution, which is pre-set to be two. At about time $3LM$, the induced current increases quickly and the adopted resolution also increases up to a maximum of six. After that, with the oscillation of the induced current, the resolution level varies. At the later time, the resolution decreases to the lowest order of two. Also observed from the results illustrated in figure 6 is that at about the first one third of the simulation duration, the adaptive result shows an accuracy very close to a fixed resolution of four. Afterwards, the accuracy degrades gradually to the lowest resolution of two.

The adaptive results showed in figures 4, 5 and 6 are computed based on linear interpolation. Similar results are also computed based on second order spline interpolation. Comparing figures 5 and 7, we will see the improvement of the smoothness in transition between different resolution levels.

By selecting proper criteria when and where to apply higher order unknowns, we can obtain better results with less computation resources. Another example is showed in figure

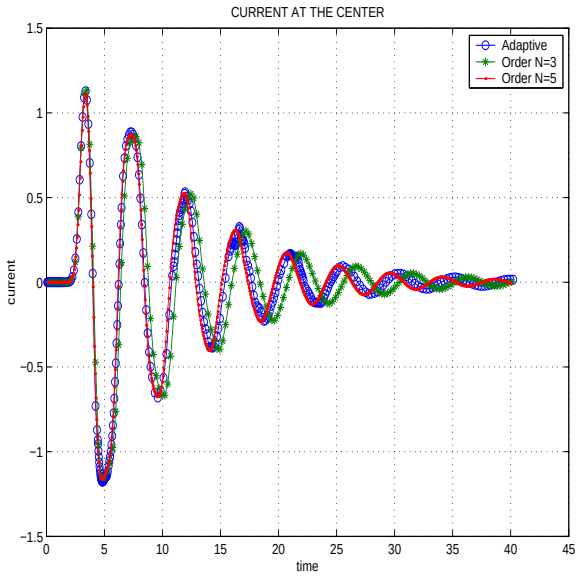

Fig. 8. transient current at the center of the wire: adaptive method gives accurate result at early time and needs less computation at later time

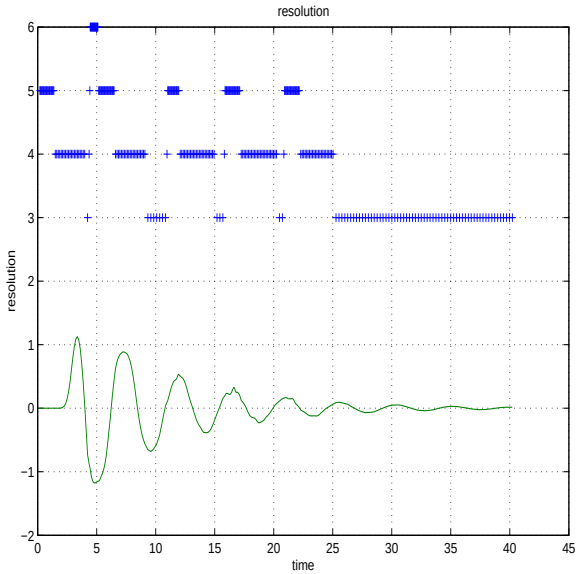

Fig. 9. Resolution distribution with time

8. We see that at the early time, the algorithm adopts higher order resolutions thus gives more accurate result. At the later time, the response is less important, thus the algorithm uses lower order resolutions and gives result with low accuracy. The distribution of the resolution levels is plotted in figure 9.

In this paper, we have not compared the computation time quantitatively. We can make a theoretical estimation for the 3-D applications. In the classical marching-on-time (MOT) methods of IETD, there are two main stages to the solution: formulation of the main system matrix, essentially relating the contribution to the field at each node made by the earlier field at each other node, and repeated stepping through time. For each time step, at each node, the field is calculated by summing the effects of the historical field values over the rest of the surface. The number of steps generally scales linearly with frequency. Therefore, the MOT scheme of IETD has complexity of $O(N_t N_s^2)$, where N_t and N_s are the numbers of temporal and spatial basis functions discretizing the scatterer current (or field), thus the cost scales with the fifth power of frequency. (The cost of the IEFD methods scales with the sixth power of frequency, arising from the need for inversion of a dense matrix, the size of which scales with the square of frequency.)

The Walker's group [18] claimed that though in their implicit approach, a sparse matrix is required to be solved at each time step, the method still gains computational economies because of the smaller number of time steps needed in the whole analysis. They further proposed an approach, based on observation of the physical characteristics of the field distributions generated by short-duration excitations, reducing the computational cost from fifth to fourth, even third power of frequency, and the storage reduced from fourth to third even second power of frequency. In their method, in which by an imposed (or even variable) threshold (although this needs some extra cost), some deemed non-active regions are ignored. Their modifications to the normal algorithm are: instead of integrating over the whole surface from each node at each time step, integrate over only that portion of the surface that can be determined to have had large fields at the particular associated historical time; only do this for those nodes at where large resultant fields are expected. By this physical approximation, they claimed that neglect of large fractions of the surface leads to only modest reductions in accuracy.

Walker's method based on physical approximation being heuristic in nature, the Michielssen's group [19], [20] has proposed a numerically rigorous scheme, based on the ideas of fast multipole method (FMM), to reduce to complexity to $O(N_t N_s^{1.5} \log N_s)$ using a two-level plane wave time-domain algorithm. The PWTD-enhanced MOT algorithm that enable the fast evaluation of transient scalar wave fields by decomposing radiated fields into transient plane waves permits fast EFIE, MFIE and CFIE based analysis of transient electromagnetic scattering phenomena and is claimed useful in characterizing broadband scattering from large objects.

V. CONCLUSIONS

This paper applies the method of moments (MOM) to the typical straight thin wire antenna. We have analyzed the induced current along the wire by using frequency domain method, ordinary time domain method and multiresolution method. Comparison is made between results computed by different methods.

Generally speaking, the input field pulse in the transient analysis has very short duration and thus broadband spectrum. We need higher order resolution to simulate the response due to the input pulse. At the later time, the resonant frequency of the structure dominates. This resonant frequency usually much lower than the input spectrum thus only a lower resolution is needed. To effectively analyze the problem, the multiresolution method is preferred. Otherwise we may miss the fast variations at the early time if a lower resolution is applied, or we may do much unnecessary work at later time if a high resolution is adopted.

One of the critical issues in the multiresolution analysis is how to determine effectively when and where to turn the high order unknowns "on" or "off". The proper "turn on" of the high order unknowns provides accuracy and the appropriate "turn off" garantees the effectiveness of the algorithm.

Wavelet basis functions have been proven to be effective in adaptive multiresolution analysis. The scaling function catches the smooth portion of the simulated variables while the wavelet functions grasp the details. By observing the scale and dilation indices, we can easily determine the characteristics of the rapid variations. This is useful in the transient analysis.

ACKNOWLEDGMENTS

The author would like to thank Professor Christos Christodoulou for his excellent lecture during the course. The author would also like to thank his supervisor, professor Scott Tyo, for his helpful discussions on the author's research, some of which contributes to parts of the project paper.

REFERENCES

[1] Andrew F. Peterson, Scott L. Ray, and Raj Mittra, *Computational methods for electromagnetics*, IEEE Press, NY, 1998.

[2] Leland Jameson,"A Wavelet-Optimized, Very High Order Adaptive Grid and Order Numerical Method," *SIAM Journal on Scientific Computing*, Volume 19, Number 6, pp. 1980-2013

[3] C. Su and T.K. Sarkar, "A Multiscale Moment Method for solving Fredholm Integral Equation of the first kind" *PIER, edited by J. A. Kong*, Vol. 17, Chap. 7, pp. 237-264, 1997

[4] C. Su and T. K. Sarkar, "Electromagnetic scattering from two-dimensional electrically large perfectly conducting objects with small cavities and humps by use of adaptive multiscale moment methods (AMMM)" *Journal of Electromagnetic Waves and Applications*, Vol.12, No. 7, pp. 885-907, 1998.

[5] Chaowei Su and T.K. Sarker, "Adaptive multiscale moment method (AMMM) for analysis of scattering from three-dimensional perfectly conducting structures," *IEEE Transactions on Antennas and Propagation*, Vol. 50, No.4, Apr., 2002, pp.444-450

[6] Dogaru, T.; Carin, L., "Application of Haar-wavelet-based multiresolution time-domain schemes to electromagnetic scattering problems," *IEEE Transactions on Microwave Theory and Techniques*, Vol. 49 No.5, May, 2001, pp.902-912

[7] L. Tarricone and F. Malucelli,"Efficient linear system solution in moment methods using wavelet expansions," *IEEE Transactions on Antennas and Propagation*, Vol. 50, No.6, June, 2002, pp.774-784

[8] E. M. Tentzeris, A. Cangellaris, L. P. B. Katehi and J. Harvey, "Multiresolution time-domain (MRTD) adaptive schemes using arbitrary resolutions of wavelets," *IEEE Transactions on Microwave Theory and Techniques*, Vol. 50, No.2, Feb, 2002, pp.501-516

[9] Xingchang Wei, Erping Li and Changhong Liang, "A new MRTD scheme based on Coifman scaling functions for the solution of scattering problems," *IEEE Microwave and Wireless Components Letters*, Vol. 12, No.10, Oct., 2002, pp.392-394

[10] O. V. Vasilyev, S. M. Paolucci and Sen,"A Multilevel Wavelet Collocation Method for Solving Partial Differential Equations in a Finite Domain," *J. Comp. Phys.*, 120, pp.33-47, 1995

[11] L. Tarricone and F. Malucelli,"Efficient linear system solution in moment methods using wavelet expansions," *IEEE Transactions on Antennas and Propagation*, Vol. 48 No.8, Aug. 2000, pp.1257 -1259

[12] S. Grivet-Takocia,"Adaptive transient solution of nonuniform multiconductor transmission lines using wavelets," *IEEE Transactions on Antennas and Propagation*, Vol. 48 No.10, Oct. 2000, pp.1563-1573

[13] Y. Shifman and Y. Leviatan, "On the use of spatio-temporal multiresolution analysis in method of moments solutions of transient electromagnetic scattering," *IEEE Transactions on Antennas and Propagation*, Vol. 49 No.8, Aug. 2001, pp.1123-1129

[14] M. Fujii and W. J. R. Hoefer, "Time-domain wavelet Galerkin modeling of two-dimensional electrically large dielectric waveguides," *IEEE Transactions on Microwave Theory and Techniques*, Vol. 49 No.5, May, 2001, pp.886-892

[15] Young Wook Cheong, Yong Min Lee, Keuk Hwan Ra, Joon Gil Kang and Chull Chae Shin, "Wavelet-Galerkin scheme of time-dependent inhomogeneous electromagnetic problems ," *IEEE Microwave and Guided Wave Letters*, Vol. 9, No.8, Aug, 1999, pp.297-299

[16] Roger F. Harrington, *Field computation by moment methods*, The macmillan Company, NY, 1968.

[17] Sadasiva M.Rao (Editor), *Time domain electromagnetics*, Academic Press, CA, 1999.

[18] M. D. Pocock, M. J. Bluck and S. P. Walker,"Electromagnetic scattering from 3-D curved dielectric bodies using time-domain integral equations," *IEEE Transactions on Antennas and Propagation*, Vol. 46 No.8, Aug. 1998, pp.1212-1219

[19] B. Shanker, A. A. Ergin, K. Aygun and E. Michielssen,"Analysis of transient electromagnetic scattering phenomena using a two-level plane wave time-domain algorithm," *IEEE Transactions on Antennas and Propagation*, Vol. 48 No.4, Apr. 2000, pp.510-523

[20] B. Shanker, A. A. Ergin, K. Aygun and E. Michielssen,"Analysis of transient electromagnetic scattering from closed surfaces using a combined field integral equation," *IEEE Transactions on Antennas and Propagation*, Vol. 48 No.7, July, 2000, pp.1064-1074

PLACE PHOTO HERE

Zhaoxian Zhou is a Ph.D candidate in the department of Electrical and Computer Engineering of University of New Mexico. His rersearch interests include computational electromagnetics, pulsed power microwaves, radio wave propagations and wireless communications.